Biophysical Journal, Volume 99

Supporting Material

Coclustering of ErbB1 and ErbB2 revealed by FRET-sensitized acceptor bleaching

Ágnes Szabó, János Szöllösi, and Peter Nagy

Supplementary material

Determination of the effect of donor photobleaching

The process of FSAB was analyzed according to the scheme in Fig. S3A. For the sake of simplicity, but without the loss of generality, donor-acceptor complexes were assumed to be dimers. Four different molecular species were assumed to exist: *DA*, D_bA, DA_b, D_bA_b, where *A* and *D* are acceptor and donor, respectively, and subscript *b* denotes bleached molecules. Three different types of transition interconvert the species to each other: donor bleaching and acceptor bleaching induced by direct acceptor excitation and by FRET (FSAB). If the rate of donor photobleaching is not negligible compared to acceptor bleaching, then acceptor molecules present in complexes in which the donor is bleached before the acceptor cannot be bleached by FSAB. The scheme presented in Fig. S3A is described by the following set of differential equations:

$$\frac{dDA(t)}{dt} = -DA(t)\ \left[S_{1A,eq}\ k_{b,A} + S_{1D,eq}\ (1-FRET)\ k_{b,D} + S_{1A,eqFRET}\ k_{b,A}\right] \quad \text{(S1)}$$

$$\frac{dDA_b(t)}{dt} = DA(t)\ \left(S_{1A,eq}\ k_{b,A} + S_{1A,eqFRET}\ k_{b,A}\right) - DA_b(t)\ S_{1D,eq}\ k_{b,D} \quad \text{(S2)}$$

$$\frac{dD_bA(t)}{dt} = DA(t)\ S_{1D,eq}(1-FRET)\ k_{b,D} - D_bA(t)\ S_{1A,eq}\ k_{b,A} \quad \text{(S3)}$$

$$\frac{dD_bA_b(t)}{dt} = DA_b(t)\ S_{1D,eq}\ k_{b,D} + D_bA(t)\ S_{1A,eq}\ k_{b,A} \quad \text{(S4)}$$

where *FRET* is the efficiency of FRET, $k_{b,D}$ and $k_{b,A}$ are the molecular bleaching rate constants of the donor and the acceptor, respectively, and $S_{1D,eq}$, $S_{1A,eq}$ and $S_{1A,eqFRET}$ are the equilibrium population probabilities of the S_1 state of the donor in the absence of FRET, the equilibrium population probability of directly excited acceptors and that of acceptors excited by FRET. Equations S1-S4 hold if the FRET efficiency is low, therefore the fractions of directly excited acceptors and those excited by FRET are additive. If the rate of excitation of a molecule is low, the equilibrium population probability is reasonably well approximated by the following formula:

$$S_{1,eq} = \frac{k_{exc}}{k_0} \quad \text{(S5)}$$

where k_{exc} and k_0 are the summed rate constants of excitation and relaxation, respectively. In the case of acceptors excited by FRET equation S5 takes the following form:

$$S_{1A,eqFRET} = \frac{S_{1D,eq}\ (1-FRET)k_{FRET}}{k_{0A}} = S_{1D,eq}\ FRET\frac{\tau_A}{\tau_D} \quad \text{(S6)}$$

where τ_A and τ_D are the fluorescence lifetimes of the acceptor and donor, respectively.

In the case of a 3-level energy system (S_0, S_1 and T_1 levels) the apparent photobleaching rate constant ($k_{b,app}$) is defined as follows (1):

$$k_{b,app} = k_b\ S_{1,eq} \quad \text{(S7)}$$

$k_{b,app}$ can be determined by fitting a mono-exponential function to the intensity vs. time plot:

$$I(t) = I_0\ e^{-k_{b,app}\ t} \quad \text{(S8)}$$

k_b can be calculated according to the following equation (1):

$$k_b = \frac{\Phi_b}{\tau} \quad \text{(S9)}$$

Using equations S6, S7 and S9 $S_{1A,eqFRET} \times k_{b,A}$ can be expressed as follows :

$$S_{1A,eqFRET}\ k_{b,A} = k_{b,app,D}\ FRET\frac{\Phi_{b,A}}{\Phi_{b,D}} \quad \text{(S10)}$$

where $\Phi_{b,D}$ and $\Phi_{b,A}$ are the photobleaching quantum yields of the donor and acceptor, respectively.

If donor bleaching is neglected, only two kinds of species exist (DA, DA_b), and the differential equation describing the process is significantly simpler:

$$\frac{dDA_b(t)}{dt} = DA(t)\ \left(S_{1A,eq}\ k_{b,A} + S_{1A,eqFRET}\ FRET\ k_{b,A}\right) \quad \text{(S11)}$$

Solving differential equation S11 and the set of differential equations S1-S4 (after substituting equations S7 and S10) by Mathematica (Wolfram Research, Champaign, IL) acceptor bleaching was compared in the presence and absence of donor bleaching for the AlexaFluor546-Cy5 pair. The apparent photobleaching rate constants of AlexaFluor546- and Cy5-conjugated antibodies bound to cells were determined experimentally by fitting the fluorescence decay curves to equation S8 ($k_{b,app,D}$=0.0367, $k_{b,app,A}$=0.16). The photobleaching quantum yields of AlexaFluor546 and Cy5 were assumed to be 8.9×10^{-5} and 3.6×10^{-5}, respectively, in the absence of CBr_4 (2, 3). Since CBr_4 differentially changes the photobleaching of the two dyes, its effect on the photobleaching quantum yields has to be considered. The photobleaching quantum yield is the reciprocal of the mean number of

survived absorption cycles, which is proportional to the total number of emitted photons before the dye bleaches (1). Since the total number of emitted photons is the area under the curve (AUC) of the fluorescence decay curve, the CBr_4 induced change in the photobleaching quantum yield can be calculated according to the following equation:

$$\frac{\Phi_{b,CBr_4}}{\Phi_{b,0}} = \frac{AUC_0}{AUC_{CBr_4}} \tag{S12}$$

We found that the photobleaching quantum yields of AlexaFluor546 and Cy5 were increased 2-fold and 95-fold, respectively, by CBr_4 when exciting the dyes at the donor excitation wavelength.

Using the aforementioned values, a FRET efficiency of 40% and assuming that half of the acceptors are bound to donors we found that bleaching of the donor negligible influences the rate of acceptor photobleaching, since the accumulation of the D_bA species is negligible and transient (Fig. S3B). In addition, the calculations showed that approximately 50% of free acceptors are bleached by the time all of the bound acceptors are photobleached. This finding is in accordance with the experimentally observed value of the bleaching correction factor (*BCF*) of ~40-50% and shows that the fraction of donor-bound acceptors can be reliable determined due to their preferential bleaching compared to free acceptors.

Determination of the effect of fixation on the lateral mobility of ErbB1

Cells and plasmids

The plasmid for ErbB1 was the kind gift of Yosef Yarden (Weizmann Institute of Science, Rehovot, Israel). Generation of the plasmid coding for ErbB1-eGFP has been described elsewhere (4). A4erbB1 cells have been established by stably transfecting subclone E3 of the A431 cell line (obtained from Ernst Helmreich, University of Würzburg) with ErbB1-eGFP (5). A4erbB1 expresses ~2×10^6 endogenous ErbB1 and ~10^6 ErbB1-eGFP as determined by flow cytometry using Qifikit (Dako-Cytomation, DAKO, Hamburg, Germany). Cells were cultured in 8-well chambered coverglass (Nalge Nunc International, Rochester, NY) for FRAP experiments.

Fluorescence recovery after photobleaching (FRAP)

A Zeiss LSM 510 confocal laser scanning microscope (Carl Zeiss AG, Jena, Germany) was used for FRAP experiments. The power of the 488 nm line of an Ar ion laser was set to 5% for imaging eGFP. Fluorescence of eGFP was recorded using a 505LP filter. The power of the 488 line was adjusted to 100% when bleaching rectangular areas (~2×2 μm) in the cell membrane, and the recovery of fluorescence was monitored by taking images every second for ~150 sec using excitation at 488 nm attenuated to 5%. Image processing was carried out with the DipImage toolbox (Delft University of Technology, Delft, The Netherlands) under Matlab (Mathworks Inc., Natick, MA). Image registration was carried out using the 'correctshift' command of DipImage followed by calculating the mean fluorescence intensity in the bleached region. Fluorescence recovery was fitted to equation S13 in Matlab:

$$a+(1-a-b)\left(1-e^{-\frac{t}{\tau}}\right) \tag{S13}$$

where τ is the empirical recovery time constant. The fraction of immobile fluorescent molecules was calculated according to equation S14:

$$\frac{b}{1-a} \tag{S14}$$

Results and discussion

The lateral mobility of ErbB1 was investigated by FRAP in A4erbB1 cells. The recovery of fluorescence in non-fixed cells revealed an apparent recovery time constant of ~10 sec and

an immobile fraction of ~55% (Fig. S3). Fixation in 1% formaldehyde under conditions similar to FSAB experiments almost completely inhibited lateral mobility of ErbB1-eGFP since the immobile fraction was increased to >90%. Addition of CBr_4 to fixed cells did not significantly modify the mobility of ErbB1-eGFP. Although several previous publications showed that the lateral mobility of transmembrane proteins is only marginally inhibited by mild (~1%) formaldehyde fixation (6, 7), our FRAP experiments conclusively showed that the fixation protocol used for FSAB experiments essentially completely prevents the diffusion of ErbB1 in the plane of the membrane during the photobleaching. Therefore, only acceptors in the immediate vicinity of a donor are expected to get photobleached by FSAB.

Supplementary references

1. Eggeling, C., J. Widengren, R. Rigler, and C. A. M. Seidel. 1999. Photostability of fluorescent dyes for single-molecule spectroscopy. In Applied Fluorescence in Chemistry, Biology and Medicine. W. Rettig, B. Strehmel, S. Schrader, and H. Seifert, editors. Springer-Verlag, Berlin. 193-240.
2. Gould, T. J., J. Bewersdorf, and S. T. Hess. 2008. A quantitative comparison of the photophysical properties of selected quantum dots and organic fluorophores. Z. Phys. Chem. 222:833-849.
3. Frederix, P. L. T. M., and E. L. de Beer. 2002. Dynamic Monte Carlo simulations to model FRET and photobleaching in systems with multiple donor-acceptor interactions. J. Phys. Chem. B 106.
4. Brock, R., I. H. Hamelers, and T. M. Jovin. 1999. Comparison of fixation protocols for adherent cultured cells applied to a GFP fusion protein of the epidermal growth factor receptor. Cytometry 35:353-362.
5. Lidke, D. S., P. Nagy, R. Heintzmann, D. J. Arndt-Jovin, J. N. Post, H. E. Grecco, E. A. Jares-Erijman, and T. M. Jovin. 2004. Quantum dot ligands provide new insights into erbB/HER receptor-mediated signal transduction. Nat Biotechnol 22:198-203.
6. Frick, M., K. Schmidt, and B. J. Nichols. 2007. Modulation of lateral diffusion in the plasma membrane by protein density. Curr Biol 17:462-467.
7. Wey, C. L., R. A. Cone, and M. A. Edidin. 1981. Lateral diffusion of rhodopsin in photoreceptor cells measured by fluorescence photobleaching and recovery. Biophys J 33:225-232.

Supplementary table

Table S1. The composition of ErbB1 and ErbB2 homoclusters and their heteroclusters in quiescent and EGF-stimulated SKBR-3 cells.

	free/homoclustered ErbB1 ($\times 10^3$)	ErbB1-ErbB2 complex ($\times 10^3$)	free/homoclustered ErbB2 ($\times 10^3$)
quiescent	120±8	80±8 ErbB1 120±24 ErbB2	1080±24
EGF-stimulated	134±10	66±10 ErbB1 252±36 ErbB2	948±36

The numbers of free (or homoclustered) and heteroclustered ErbB proteins (±standard error of the mean) determined by FSAB are rearranged compared to Table 1 in order to emphasize the composition of ErbB1-2 heteroclusters.

Supplementary figures

Figure S1. The effect of CBr_4 on the photobleaching rate of potential donors and acceptors.

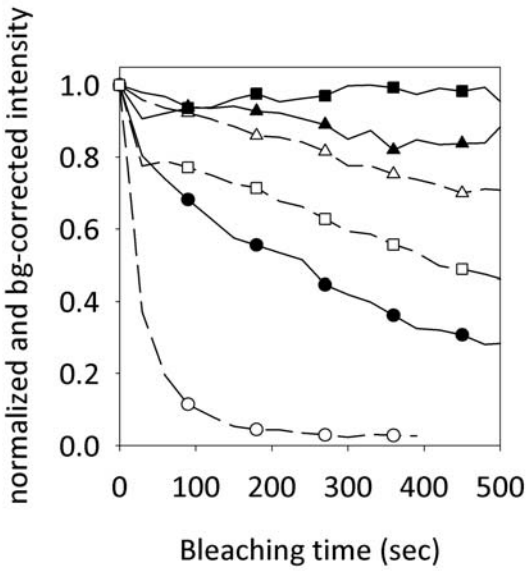

SKBR-3 cells labeled by trastuzumab tagged with AlexaFluor546 (▲,△), Qdot605 (■,□) or Cy5 (●,○) were photobleached by illuminating the samples at 543 nm (AlexaFluor546, Qdot605) or 633 nm (Cy5). Images were recorded by interrupting the bleaching illumination every ~30 sec. Photobleaching was carried out in the absence (filled symbols) or presence (empty symbols) of CBr_4. Symbols are shown for every third measurement point for easier discernability.

Figure S2. Wavelength-dependent photobleaching of Cy5.

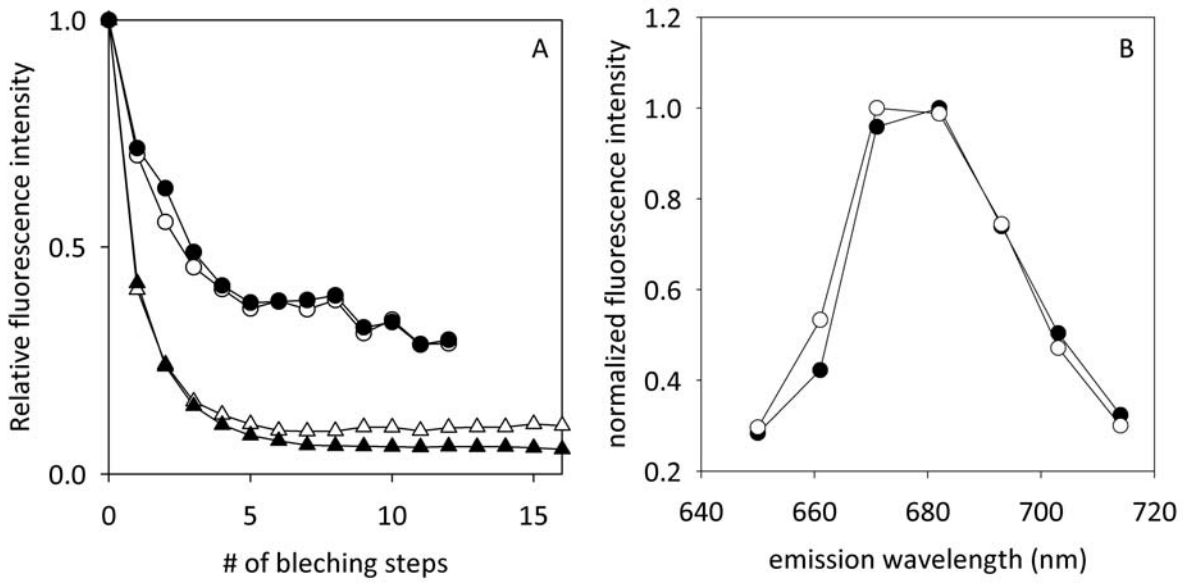

A. SKBR-3 cells labeled by Cy5-trastuzumab were photobleached at 543 nm and the fluorescence intensity of Cy5 was measured at an excitation wavelength of 543 nm (○) or 633 nm (●) using an attenuated laser beam when interrupting the bleaching illumination. Cy5-trastuzumab-labeled SKBR-3 cells were photobleached by illuminating them at 633 nm, and their fluorescence intensity was recorded at an excitation wavelength of 543 nm (△) or 633 nm (▲). The emission of Cy5 was measured using a 650 nm long-pass filter.

B. The emission spectra of Cy5 excited at 633 nm were recorded on an unbleached sample (●) and on a sample bleached at 543 nm (○). The measurement was carried out at a resolution of 10 nm on cells attached to glass coverslips using the Meta unit of a Zeiss LSM510 confocal microscope.

Figure S3. Bleaching of the donor has negligible effect on the rate of FRET-sensitized acceptor bleaching.

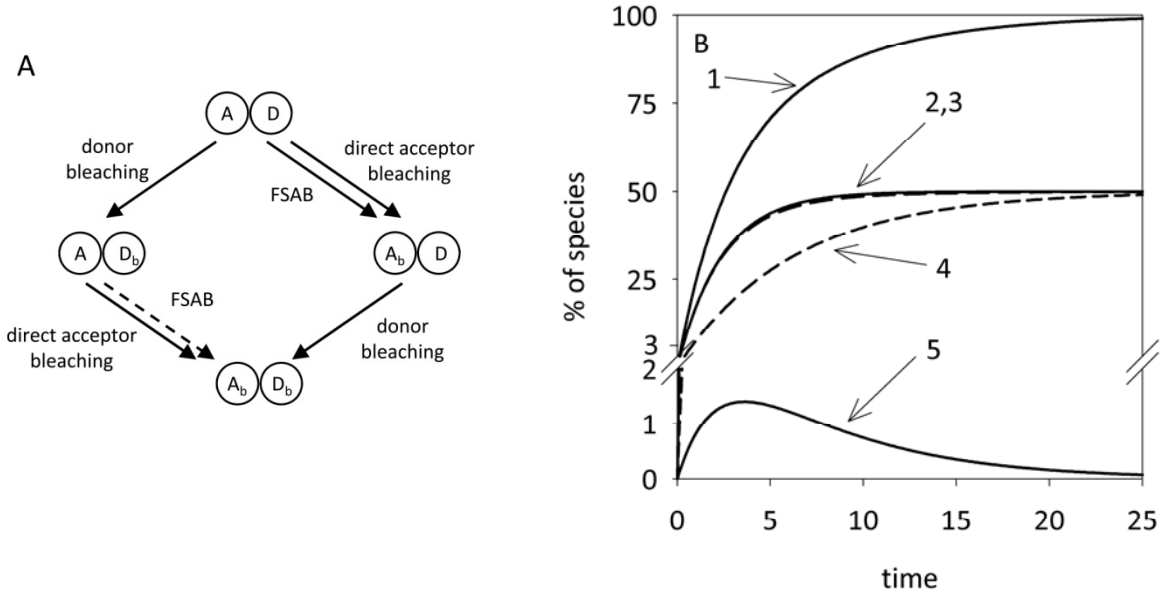

A. Reaction scheme of a donor-acceptor dimer undergoing FRET-sensitized acceptor bleaching. Letters *A* and *D* stand for the acceptor and donor, respectively. Subscript b indicates a bleached molecule. If a donor is bleached before the acceptor in a heterodimer, that acceptor cannot be bleached by FSAB indicated by the dashed arrow.

B. The sets of differential equations describing direct and FRET-sensitized bleaching of the acceptor with (equations S1-S4) and without (equation S11) donor bleaching were solved with the parameters described in the Theory section. A 50-50% mixture of free and donor-bound acceptors was assumed. The percentages of bleached acceptors (free+bound, curve 1), bound and bleached acceptors in the presence (curve 2) and absence (curve 3) of donor bleaching, free and bleached acceptors (curve 4) and the transient accumulation of the D_bA species (complex of a bleached donor and an unbleached acceptor, curve 5) are shown in the figure.

Figure S4. Formaldehyde fixation immobilizes ErbB1 expressed in the cell membrane.

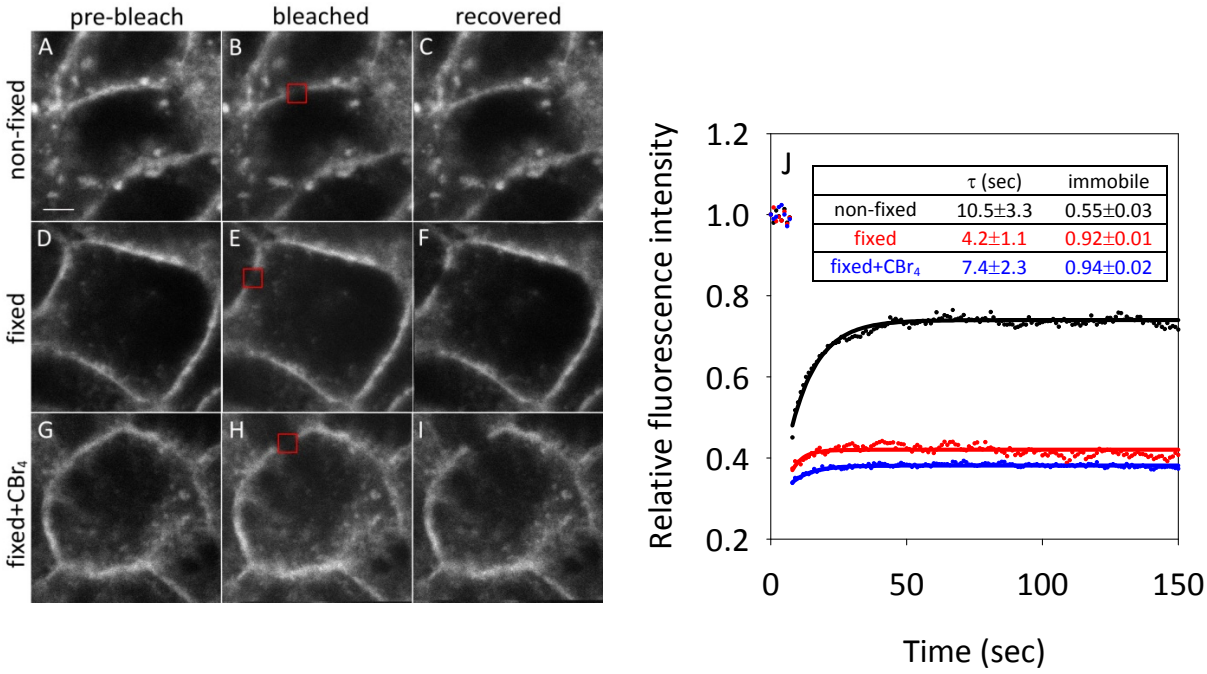

A-I. Rectangular areas in the membrane of A4erbB1 cells were photobleached and the recovery of fluorescence was monitored by confocal microscopy. The experiment was carried out with non-fixed cells (A-C, black curve in J), cells fixed in 1% formaldehyde (D-F, red curve in J) and with fixed cells treated with CBr_4 (G-H, blue curve in J). "Pre-bleach", "bleached" and "recovered" images were taken before and immediately after the bleaching and at the end of the observation period (150 sec), respectively. The bleached regions are marked by the red rectangles. The scale bar in A is 5 μm.

J. Representative FRAP curves for non-fixed (black), fixed (red) and CBr_4-treated fixed cells (blue). The dotted lines display the measured fluorescence intensity values, and the continuous ones are curves fitted to equation S13. The inserted table shows the means (±standard error of the mean) of the recovery time constants and the fraction of immobile ErbB1-eGFP calculated from five independent measurements.

Figure S5. Measured and calculated dependence of the FRET efficiency and clustered acceptors on the expression levels of the donor and acceptor.

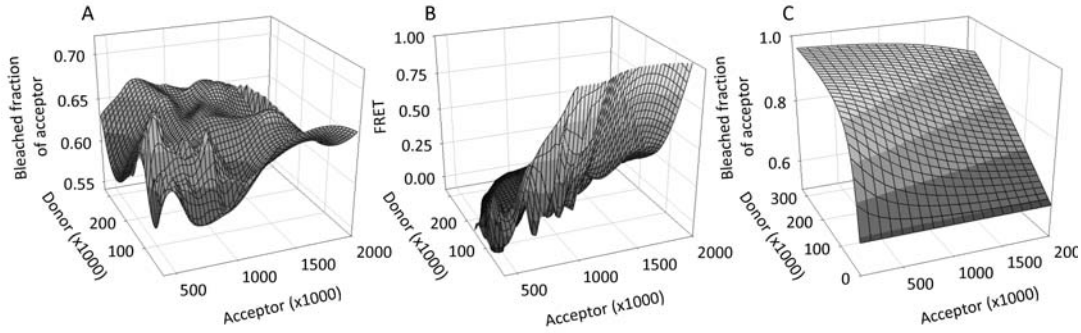

A-B. SKBR-3 cells were labeled by a mixture of AlexaFluor546-Mab528 and Cy5-trastuzumab against ErbB1 and ErbB2, respectively. The fraction of ErbB2 heteroclustering with ErbB1 (bleached fraction of acceptor) determined by FSAB (A) and the FRET efficiency (B) are plotted as a function of the expression levels of the donor and acceptor in single cells. The graphs contain the data of ~100 cells.

C. The expected fraction of bleached (clustered) acceptors calculated according to the law of mass action assuming that six acceptors bind a single donor, a K_d of 10^5 and a bleaching correction factor (*BCF*) of 0.6.